Nebojša Zdravković
Teaching Assistant
University of Kragujevac
Faculty of Mechanical and Civil Engineering
in Kraljevo, Serbia

Milomir Gašić
Professor
University of Kragujevac
Faculty of Mechanical and Civil Engineering
in Kraljevo, Serbia

Mile Savković
Professor
University of Kragujevac
Faculty of Mechanical and Civil Engineering
in Kraljevo, Serbia

Goran Marković
Assistant Professor
University of Kragujevac
Faculty of Mechanical and Civil Engineering
in Kraljevo, Serbia

Goran Bošković
PhD Student
University of Kragujevac
Faculty of Mechanical and Civil Engineering
in Kraljevo, Serbia

Finite difference scheme for free bending vibration of elastically supported non-uniform cantilever beam with lumped mass at the tip

Differential eigenvalue problem of tapered cantilever beam with tip mass and elastically restrained root was solved efficiently and accurately by building a compact structure of algebraic equations, based on finite difference method. Exact differential governing equation and boundary conditions were discretized with central differences applied upon grid points along the beam. Influence of support rigidity on mode shape function was discussed in term of discretized boundary equation. Boundary value problem was transformed in an appropriate matrix form, suitable for development of computational algorithm and solving with MATLAB routines. For a comparison purpose, a finite element method analysis was conducted in ANSYS. Testing cases were set up for numerous values of non-dimensional stiffness and mass parameters. Presented model yielded circular natural frequencies that were in a very good agreement with the results obtained from finite element simulation.

Keywords: *finite difference method, Euler–Bernoulli theory, tapered cantilever beam, elastic root, tip mass, eigenvalue.*

1. INTRODUCTION

The extensive study of free bending vibration of non-uniform flexible beams started back few decades ago [1-5]. Since then, the issue of natural frequencies in bending vibrations of non-uniform flexible beams with various boundary conditions was studied in numerous cases and by different approaches and methods. Zhou and Cheung [6] developed a new set of beam functions as admissible functions in order to obtain eigenfrequency equation by the Rayleigh-Ritz method, while Auciello [7] used Rayleigh-Ritz and Lagrangian approaches to define the upper and the lower bonds for natural frequencies of tapered beam subjected to constant axial load. Naguleswaran [8-9] used analytical method and continuity of deflection, slope, bending moment and shearing force to calculate the frequencies of beams with up to three step changes in cross-section. Li et al. [10] developed a finite element with generalized degrees of freedom for the dynamic analyses of beams and plates with cross-section varying in a continuous or discontinuous manner. Qiao et al. [11] presented analytical method for investigating free flexural vibrations of non-uniform multi-step Euler–Bernoulli beams with any kind of support configurations and carrying an arbitrary number of single-degree-of-freedom and two-degree-of-freedom spring–mass systems.

Wu and Chen [12] derived the exact solution for the natural frequencies of an immersed elastically restrained wedge beam carrying an eccentric tip mass with mass moment of inertia.

Koplow et al. [13] found an analytical solution for the dynamic response of a discontinuous beam with one-step change. Firouz-Abadi et al. [14] used third order Wentzel-Kramers-Brillouin approximation to obtain asymptotic solution to transverse free vibrations of variable-section beams. Jaworski and Dowell [15] considered the accuracy and convergence of the Rayleigh–Ritz method, component modal analysis, and the finite element method in the free vibration analysis of a multiple-stepped cantilevered beam. Abdel-Jaber et al. [16] analyzed an elastically restrained tapered cantilever beam using the harmonic balance and the time transformation methods. Hsu et al. [17] used the Adomian modified decomposition method to obtain natural frequencies and mode shapes of non-uniform Euler–Bernoulli beam under various supporting conditions. Sapountzakis and Panagos [18] did the nonlinear analysis of beams of variable cross section, including shear deformation effect by means of boundary element method. Huang and Li [19] transformed the governing equation with varying coefficients to Fredholm integral equations and obtained natural frequencies by requiring that the resulting Fredholm integral equation has a non-trivial solution. Sarkar and Ganguli [20] assumed a prescribed polynomial as the fundamental mode shape, which satisfied the boundary conditions of a non-uniform free–free beam. They used the inverse problem approach to show that for certain mass and stiffness distributions of the beam there exists a simple closed-form solution given by the assumed polynomial. Rajasekaran [21] studied the free vibration of axially functionally graded

Correspondence to: Nebojša Zdravković, teaching assistant
Faculty of Mechanical and Civil Engineering,
Dositejeva 19, 36000 Kraljevo, Serbia
E-mail: zdravkovic.n@mfkv.kg.ac.rs

non-uniform beams with different boundary conditions using differential transformation based dynamic stiffness approach.

Yet, a fast-growing industry and infrastructure development force the mechanical and civil engineers to response promptly to new challenges in structural design with efficient but acceptably accurate solutions. At the same time, real-life tasks with their complexity usually impose the use of numerical approaches. Survey upon available literature revealed the fact that the finite difference method (FDM) was not employed as often as it deserved to be. AL-Sadder and AL-Rawi [22] used FDM for static large-deflection analysis of non-prismatic cantilever beams subjected to different types of continuous and discontinuous loadings, while Awrejcewicz et al. [23] studied regular and chaotic dynamics of the uniform Euler-Bernoulli beams and used FDM and finite element method (FEM) to verify the reliability of the obtained results.

This paper presents a detailed workflow of the FDM application to the eigenvalue problem of the non-uniform beam in bending vibration. Presented approach yields a numerical scheme suitable for development of computational algorithms that enable quick and acceptably accurate dynamic analysis in terms of non-dimensional parameters. Accuracy of the obtained results is verified by FEM analysis and the results are in a very good agreement.

2. MODEL DESCRIPTION AND GOVERNING EQUATION

The model of tapered cantilever beam with tip mass and elastically restrained root considered herein is depicted in Fig.1. The motion under consideration is a free bending vibration of the beam in its symmetry plane *xy*. Transverse and axial displacements at supported end are fully restrained, while rotational restraint is elastic and presented by rotational spring with constant stiffness *k*. A lumped mass *M* is attached at the free end of the beam. The beam has a rectangular hollow cross-section with constant width *B* and wall thickness δ, while height *H(x)* linearly decreases towards its free end. Consequently, we have beam mass per unit length *m(x)* and the flexural rigidity *EI(x)* varying along length *L*, where *E* is Young's modulus of elasticity and *I(x)* is the cross-sectional moment of inertia about an axis normal to *x* and *y* and passing through the center of the cross section. The beam height in its root (*x=0*) is denoted as H_0, while the free end height (*x=L*) is denoted as H_L.

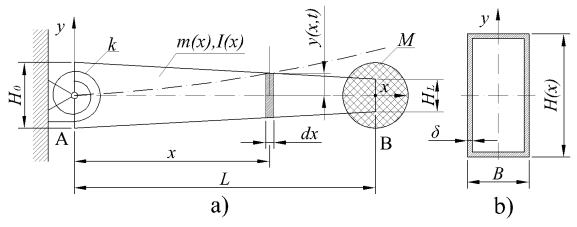

Figure 1. a Tapered cantilever beam model with elastically restrained root and tip mass b Cross-section

Analysis relies on Euler-Bernoulli beam theory, i.e. on the assumption that the rotatory inertia of the differential element and shear effects are negligible. The partial differential equation of motion for the free vibration of beams in bending, according to Euler-Bernoulli beam theory, is well known [24]

$$-\frac{\partial^2}{\partial x^2}\left[EI(x)\frac{\partial^2 y(x,t)}{\partial x^2}\right]=m(x)\frac{\partial^2 y(x,t)}{\partial t^2} \qquad (1)$$

$$0\le x\le L$$

After differentiation, expanded form of (1) is

$$-E\left[\frac{d^2I(x)}{dx^2}\frac{\partial^2 y(x,t)}{\partial x^2}+2\frac{dI(x)}{dx}\frac{\partial^3 y(x,t)}{\partial x^3}+ I(x)\frac{\partial^4 y(x,t)}{\partial x^4}\right]=m(x)\frac{\partial^2 y(x,t)}{\partial t^2} \qquad (2)$$

Free vibration is harmonic, so the transverse displacement of the beam can be expressed in the form

$$y(x,t)=CY(x)\cos(\omega t-\varphi),\ 0\le x\le L \qquad (3)$$

where *C* is amplitude, *Y(x)* is a mode shape function, ω is circular natural frequency and φ is a phase angle. Inserting (3) into (2) and dividing through by *Ccos(ωt-φ)*, we obtain the differential eigenvalue problem for Euler-Bernoulli non-uniform beam in bending

$$E\left[\frac{d^2I(x)}{dx^2}\frac{d^2Y(x)}{dx^2}+2\frac{dI(x)}{dx}\frac{d^3Y(x)}{dx^3}+ I(x)\frac{d^4Y(x)}{dx^4}\right]=m(x)\omega^2Y(x) \qquad (4)$$

At this moment, it is useful to point that, though the chosen non-uniform beam shape is consistent with numerous engineering design applications, this approach is applicable in any other case with any other cross section type and its variation along beam length.

In this case, the height of the tapered beam cross-section at the position of the differential element is

$$H(x)=H_0-\eta x \qquad (5)$$

where

$\eta=(H_0-H_L)/L=H_L(\psi-1)/L$ is non-dimensional height decrement and $\psi=H_0/H_L$ is a taper ratio. Therefore, the cross-sectional area becomes

$$A(x)=BH(x)-(B-2\delta)\left[H(x)-2\delta\right]= =2\delta(H_0-\eta x+B-2\delta) \qquad (6)$$

and the mass per unit length, where ρ is material density, has the form

$$m(x)=2\rho\delta(H_0-\eta x+B-2\delta) \qquad (7)$$

Ignoring small quantities of higher order, the cross-sectional moment of inertia reduces to

$$I(x)\approx\frac{\delta}{6}\left[(H_0-\eta x-2\delta)^3+3B(H_0-\eta x-\delta)^2\right] \qquad (8)$$

After finding the needed derivatives out of (8) and inserting them and (7) into (4), we obtain a fully expanded differential governing equation for the beam under consideration

$$\left[(H_0-\eta x-2\delta)^3+3B(H_0-\eta x-\delta)^2\right]\frac{d^4Y}{dx^4}-$$
$$-6\eta\left[(H_0-\eta x-2\delta)^2+2B(H_0-\eta x-\delta)\right]\frac{d^3Y}{dx^3}+$$
$$+6\eta^2(H_0+B-\eta x-2\delta)\frac{d^2Y}{dx^2}- \quad (9)$$
$$-\frac{12\rho\omega^2}{E}(H_0+B-\eta x-2\delta)Y=0$$

3. BOUNDARY CONDITIONS

The solution of (9) must satisfy two boundary conditions at each end. To obtain equations of boundary conditions in term of displacement *y(x,t)*, we recall the displacement relations to bending moment *M(x,t)* and shearing force *Q(x,t)* from mechanics of materials

$$M(x,t)=EI(x)\frac{\partial^2 y(x,t)}{\partial x^2}$$
$$Q(x,t)=-\frac{\partial}{\partial x}\left[EI(x)\frac{\partial^2 y(x,t)}{\partial x^2}\right] \quad (10)$$

At the supported end, the displacement function *y(x,t)* has a zero value, while its slope outcomes from a ratio between bending moment and stiffness of the rotational spring

$$y(0,t)=0 \quad (11)$$

$$\frac{\partial y(x,t)}{\partial x}=\frac{M(x,t)}{k}=\frac{E}{k}I(x)\frac{\partial^2 y(x,t)}{\partial x^2},x=0 \quad (12)$$

Assuming that moment of inertia of attached mass *M* about an axis normal to *x* and *y* is negligible, two boundary conditions for free end are as follows

$$M(x,t)=EI(x)\frac{\partial^2 y(x,t)}{\partial x^2}=0,x=L \quad (13)$$

$$Q(x,t)=-\frac{\partial}{\partial x}\left[EI(x)\frac{\partial^2 y(x,t)}{\partial x^2}\right]=$$
$$=-M\frac{\partial^2 y(x,t)}{\partial t^2},x=L \quad (14)$$

All boundary conditions written in term of mode shape function *Y(x)* and its derivatives are

$$Y(0)=0 \quad (15)$$

$$Y'(0)=\frac{EI_0}{k}Y''(0) \quad (16)$$

$$Y''(L)=0 \quad (17)$$

$$\frac{dI(L)}{dx}Y''(L)+I(L)Y'''(L)+\frac{M\omega^2}{E}Y(L)=0 \quad (18)$$

where $I_0=I(x=0)$ and $I_L=I(x=l)$ are cross-sectional moments of inertia at the root and free end of the beam, respectively.

4. DISCRETIZATION OF BOUNDARY VALUE PROBLEM BY CENTRAL FINITE DIFFERENCES

Fig. 2 shows central finite difference grid scheme where the length of the beam *L* is equally divided by *n*+1 grid points into *n* segments with length $\Delta s=L/n$. To apply the method, there are three fictitious grid points added to the scheme, one before the root grid point and two after free-end grid point.

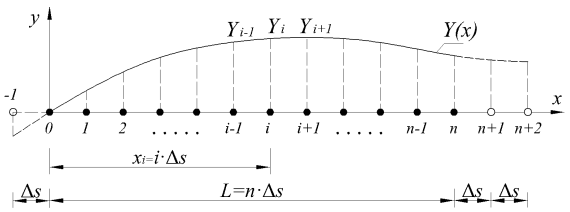

Figure 2. Central finite difference grid scheme used for discretization of boundary value problem

Central finite difference approximations for derivatives of shape function *Y(x)* for grid point *i* are as follows

$$\left(\frac{dY}{dx}\right)_i=Y_i'\approx\frac{-Y_{i-1}+Y_{i+1}}{2\Delta s} \quad (19)$$

$$\left(\frac{d^2Y}{dx^2}\right)_i=Y_i''\approx\frac{Y_{i-1}-2Y_i+Y_{i+1}}{(\Delta s)^2} \quad (20)$$

$$\left(\frac{d^3Y}{dx^3}\right)_i=Y_i'''\approx\frac{-Y_{i-2}+2Y_{i-1}-2Y_{i+1}+Y_{i+2}}{2(\Delta s)^3} \quad (21)$$

$$\left(\frac{d^4Y}{dx^4}\right)_i=Y_i^{IV}\approx\frac{Y_{i-2}-4Y_{i-1}+6Y_i-4Y_{i+1}+Y_{i+2}}{(\Delta s)^4} \quad (22)$$

4.1 Governing equation

Inserting (19-22) into the governing equation (9) and putting $x=i\cdot\Delta s$, we obtain

$$2E\left[(H_0-\eta i\Delta s-2\delta)^3+3B(H_0-\eta i\Delta s-\delta)^2\right]\cdot$$
$$\cdot(Y_{i-2}-4Y_{i-1}+6Y_i-4Y_{i+1}+Y_{i+2})-$$
$$-6\eta\Delta sE\left[(H_0-\eta i\Delta s-2\delta)^2+2B(H_0-\eta i\Delta s-\delta)\right]\cdot \quad (23)$$
$$\cdot(-Y_{i-2}+2Y_{i-1}-2Y_{i+1}+Y_{i+2})+$$
$$+12\eta^2(\Delta s)^2E(H_0-\eta i\Delta s-2\delta+B)(Y_{i-1}-2Y_i+Y_{i+1})-$$
$$-24\rho\omega^2(\Delta s)^4(H_0-\eta i\Delta s-2\delta+B)Y_i=0;\ i=1,\ldots,n$$

Eq. (23) represents a system of *n* linear algebraic equations, with discreet values of shape function at the grid points positions Y_i as unknowns. Furthermore, by introducing the expressions

$$P_i=2E\left[(H_0-\eta i\Delta s-2\delta)^3+3B(H_0-\eta i\Delta s-\delta)^2\right]$$
$$Q_i=6\eta\Delta sE\left[(H_0-\eta i\Delta s-2\delta)^2+2B(H_0-\eta i\Delta s-\delta)\right] \quad (24)$$
$$R_i=12\eta^2(\Delta s)^2E(H_0-\eta i\Delta s-2\delta+B)$$
$$S_i=24\rho(H_0-\eta i\Delta s-2\delta+B)$$

and parameter $\lambda=\omega^2(\Delta s)^4$, we rewrite (23) in more condensed form

$$(P_i+Q_i)Y_{i-2}-(4P_i+2Q_i-R_i)Y_{i-1}+$$
$$+(6P_i-2R_i-\lambda S_i)Y_i-$$
$$-(4P_i-2Q_i-R_i)Y_{i+1}+$$
$$+(P_i-Q_i)Y_{i+2}=0;\ i=1,...,n \tag{25}$$

Displacements Y_{-1}, Y_{n+1} and Y_{n+2} from equations written for grid points $i=1$ and $i=n$, which correspond to fictitious grid points added to the scheme in Fig. 2, are to be eliminated through discretization of boundary conditions.

4.2 Boundary conditions

By inserting (19-22) into (15-18), we establish the expressions for fictitious grid points displacements in terms of displacements of real grid points at the boundaries. Hence, this will enable their elimination from the system later on. Those expressions are

$$Y_0=0 \tag{26}$$

$$Y_{-1}=-\frac{2EI_0-k\Delta s}{2EI_0+k\Delta s}Y_1 \tag{27}$$

$$Y_{n+1}=2Y_n-Y_{n-1} \tag{28}$$

$$Y_{n+2}=Y_{n-2}-4Y_{n-1}+\left[4-\frac{2\omega^2(\Delta s)^3M}{EI_L}\right]Y_n \tag{29}$$

Equation (27) reveals the nature of support at the root of the beam in term of rotational spring stiffness k. Thus, if $k\to\infty$, (27) reduces to $Y_{-1}=Y_1$, which means that mode shape function $Y(x)$ has a local extreme in grid point $i=0$, i.e. $dY/dx=0$. This condition corresponds to a clamped support type. On the opposite, for $k\to 0$ we have $Y_{-1}=-Y_1$, which stands for a pinned support type. Fig. 3 represents a graphical illustration for those two cases with extreme values of parameter k. In real life, parameter k takes its value in between.

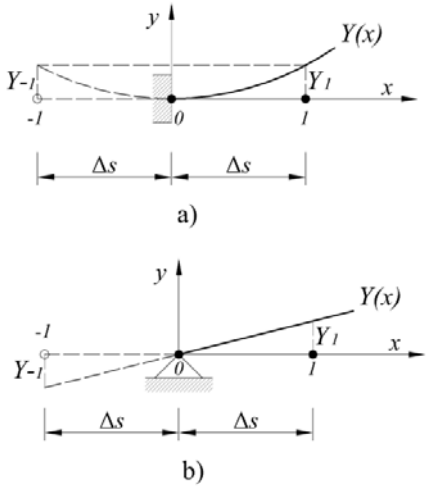

Figure 3. Mode shape function around the root in two extreme cases a $k\to\infty$ b $k\to 0$

4.3 Characteristic equation

Converting the constituent differential equations through discretization, we combine them and form the algebraic eigenvalue problem. In fact, by insertion of boundary conditions (26-29) into (25) we eliminate fictitious displacements Y_{-1}, Y_{n+1} and Y_{n+2}, which yields a set of n algebraic equations with Y_i, $i=1,...,n$ as unknowns and λ as a parameter. Boundary conditions affect the form of equations for first two and last two grid points only, while equations for all other internal grid points retain general form presented by (25)

$$i=1\to\left[6P_1-2R_1-\lambda S_1-\frac{2EI_0-k\Delta s}{2EI_0+k\Delta s}(P_1+Q_1)\right]Y_1-$$
$$-(4P_1-2Q_1-R_1)Y_2+(P_1-Q_1)Y_3=0$$
$$i=2\to-(4P_2+2Q_2-R_2)Y_1+(6P_2-2R_2-\lambda S_2)Y_2-$$
$$-(4P_2-2Q_2-R_2)Y_3+(P_2-Q_2)Y_4=0$$
$$i=3\div n-2\to(P_i+Q_i)Y_{i-2}-(4P_i+2Q_i-R_i)Y_{i-1}+$$
$$+(6P_i-2R_i-\lambda S_i)Y_i-$$
$$-(4P_i-2Q_i-R_i)Y_{i+1}+(P_i-Q_i)Y_{i+2}=0 \tag{30}$$
$$i=n-1\to(P_{n-1}+Q_{n-1})Y_{n-3}-(4P_{n-1}+2Q_{n-1}-R_{n-1})Y_{n-2}+$$
$$+(5P_{n-1}-2R_{n-1}-\lambda S_{n-1}+Q_{n-1})Y_{n-1}-(2P_{n-1}-R_{n-1})Y_n=0$$
$$i=n\to 2P_nY_{n-2}-4P_nY_{n-1}+$$
$$+\left[2(1-\frac{M\lambda}{\Delta sEI_L})P_n-\lambda S_n+\frac{2M\lambda}{\Delta sEI_L}Q_n\right]Y_n=0$$

We introduce following expressions

$$T=\frac{2EI_0-k\Delta s}{2EI_0+k\Delta s} \tag{31}$$

$$J=\frac{2M}{\Delta sEI_L}(P_n-Q_n) \tag{32}$$

to simplify and rearrange (30) to a new form

$$\frac{1}{S_1}\{[6P_1-2R_1-T(P_1+Q_1)]Y_1-$$
$$-(4P_1-2Q_1-R_1)Y_2+(P_1-Q_1)Y_3\}=\lambda Y_1$$
$$\frac{1}{S_2}\{-(4P_2+2Q_2-R_2)Y_1+2(3P_2-R_2)Y_2-$$
$$-(4P_2-2Q_2-R_2)Y_3+(P_2-Q_2)Y_4\}=\lambda Y_2$$
$$\frac{1}{S_i}\{(P_i+Q_i)Y_{i-2}-(4P_i+2Q_i-R_i)Y_{i-1}+2(3P_i-R_i)Y_i- \tag{33}$$
$$-(4P_i-2Q_i-R_i)Y_{i+1}+(P_i-Q_i)Y_{i+2}\}=\lambda Y_i$$
$$\frac{1}{S_{n-1}}\{(P_{n-1}+Q_{n-1})Y_{n-3}-(4P_{n-1}+2Q_{n-1}-R_{n-1})Y_{n-2}+$$
$$+(5P_{n-1}-2R_{n-1}+Q_{n-1})Y_{n-1}-(2P_{n-1}-R_{n-1})Y_n\}=\lambda Y_{n-1}$$
$$\frac{1}{S_n+J}(2P_nY_{n-2}-4P_nY_{n-1}+2P_nY_n)=\lambda Y_n$$

Previous form is convenient to formulate the eigenvalue problem as a matrix equation

$$\mathbf{AY}=\lambda\mathbf{Y} \tag{34}$$

i.e.

$$\left(\mathbf{A} - \lambda \mathbf{I}_n\right)\mathbf{Y} = 0 \tag{35}$$

where $\boldsymbol{A}$ is a diagonal matrix, I_n is a unit matrix of size n, λ is an eigenvalue and $\boldsymbol{Y}$ is a column matrix of displacements that form mode shape. Nontrivial solutions exist if and only if the determinant of the coefficients is equal to zero, which finally leads to characteristic equation

$$\Delta(\lambda) = \det\left[\mathbf{A} - \lambda \mathbf{I}_n\right] = 0 \tag{36}$$

Finding the roots λ_i, $i=1,\ldots,n$ of (36) we find circular natural frequencies of the beam

$$\omega_i = \frac{\sqrt{\lambda_i}}{(\Delta s)^2} = \frac{n^2\sqrt{\lambda_i}}{L^2}, i = 1,\ldots n \tag{37}$$

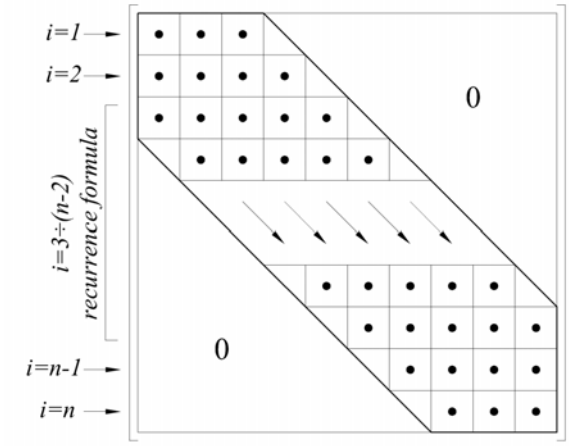

Figure 4. Matrix *A* populating scheme based on Eqs. (33)

5. NUMERICAL CALCULUS AND RESULTS COMPARISON WITH FINITE ELEMENT MODEL

To investigate the accuracy of results obtained by FDM, a calculation is carried out through numerical example with following parameters: $L=3m$, $H_L=0.1m$, $\Psi=2.0$, $B=0.1m$, $\delta=0.005m$, $\rho=7850kg/m^3$, $E=2.1\cdot10^{11}N/m^2$. The length of the beam is divided by $n=100$ grid points. As it is more convenient to analyze the results in terms of relations of the quantities rather than in terms of themselves, we introduce the following stiffness and mass non-dimensional ratios

$$q = \frac{kL}{EI_0} \tag{38}$$

and

$$r = \frac{M}{m} \tag{39}$$

where $m = \delta\rho L\left[(1+\psi)H_L + 2B - 4\delta\right]$ is the self-mass of the beam. Hence, the expressions (31-32) derived from boundary conditions now become

$$T = \frac{2n-q}{2n+q} \tag{40}$$

and

$$J = \frac{2rm}{\Delta s EI_L}(P_n - Q_n) \tag{41}$$

Numerical calculations within FDM approach were carried out by MATLAB software routines. On the other hand, we used a FEM analysis and ANSYS software to verify the results. 3-D model of the beam was discretized by automatic mesh of 28335 nodes and 4794 hexagonal finite elements. The boundary conditions were applied by elastic support, i.e. foundation stiffness at the root and point mass attached at the tip of the tapered beam model. The numerical investigation was conducted in a manner where the value of stiffness ratio was gradually increased while mass ratio took values $r=0.5;1.0;1.5;2.0$ repeatedly for each instance of stiffness ratio. Fig. 5 shows first three mode shapes and natural frequencies of the tapered beam in FEM analysis for the case where non-dimensional ratios take values $q=3.0$ and $r=0.5$. Frequencies obtained from ANSYS present number of cycles per second. Hence, they were multiplied by 2π to get circular natural frequencies for comparison with FDM results.

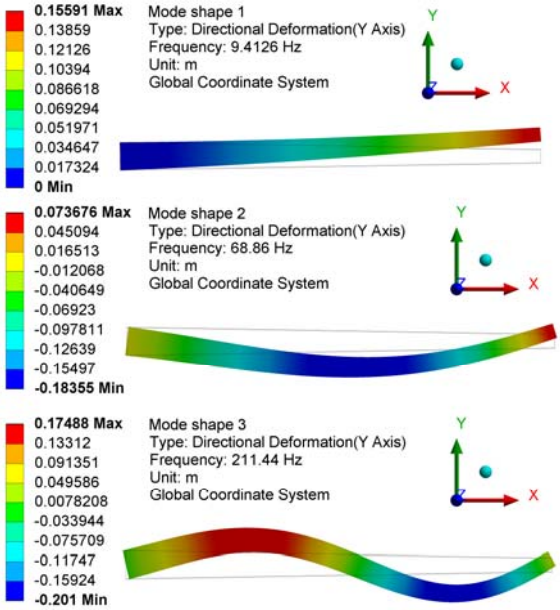

Figure 5. First three mode shapes and natural frequencies from ANSYS for *q=3.0* and *r=0.5*

Table 1 shows the results for the first three circular natural frequencies obtained by both FDM and FEM analysis and corresponding relative deviations (columns $\Delta_1, \Delta_2, \Delta_3$). A comparison between the results obtained by presented FDM approach and FEM analysis reveals very good agreement. Relative deviation for fundamental circular natural frequency does not exceed 0.19%, while for the second and third frequency it goes up to 2.15% and 5.97%, respectively.

Since the effects of rotary inertia and shear deformation are neglected in the Euler–Bernoulli beam theory, the Euler–Bernoulli model always overestimates the natural frequency of free vibration [25].

It is important to notice that, although small, relative deviations increase with growth of stiffness ratio q and reach stated maximum values for the case where parameter T, formulated by (40), is zero. Since the adopted number of segments in FDM analysis is n=100, corresponding value for non-dimensional stiffness ratio

for this case is $q=200$. Cases with $q=10^6$ and $q=10^{12}$ are added in order to reveal tendency of stabilization of relative deviation.

Figs. 6, 7 and 8 are graphical representations of the results obtained by FDM approach, i.e. the dependencies of first three circular natural frequencies on various boundary conditions in terms of non-dimensional stiffness and mass ratios q and r. Increasing the value of stiffness ratio q makes the boundary condition at the root of the beam progressively approach the clamped support type, which results in higher circular natural frequencies. Simultaneously, as expected, higher values of ratio between tip mass and self-mass of the beam r make circular natural frequencies decrease.

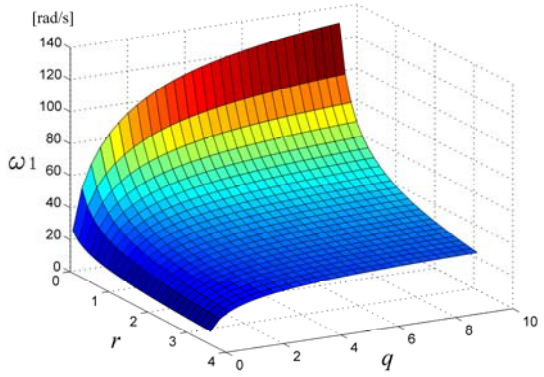

Figure 6. Influence of boundary conditions on fundamental circular natural frequency

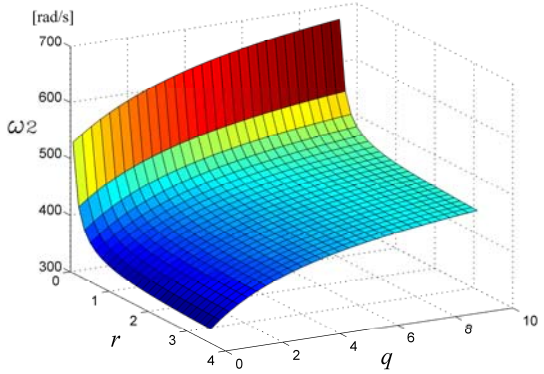

Figure 7. Influence of boundary conditions on second circular natural frequency

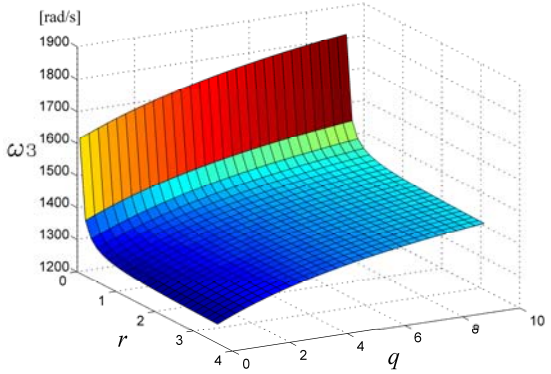

Figure 8. Influence of boundary conditions on third circular natural frequency

Fig. 9 presents a 2-D form of diagram from Fig. 6, complemented with FEM simulation results. The lines are the dependencies of the first circular natural frequency obtained from FDM approach, while markers stand for FEM simulation results given in Table 1. The results obtained from mentioned methods are in a very good agreement.

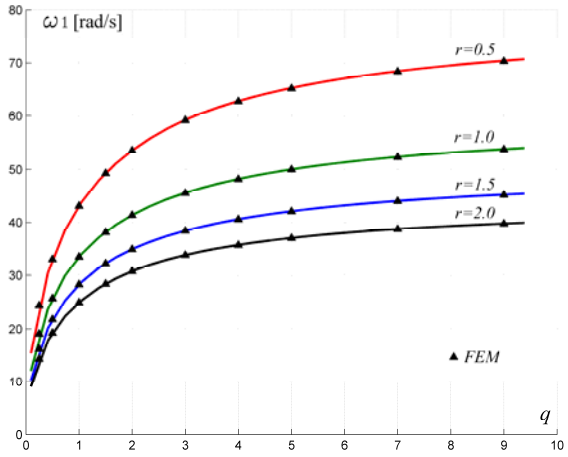

Figure 9. Comparison of results for first circular natural frequency

6. CONCLUSION

Differential eigenvalue problem of tapered cantilever beam with elastically restrained root and tip mass was efficiently solved by building a stable and compact structure of algebraic equations derived from FDM approach. The results for first three circular natural frequencies revealed very good agreement with the results obtained by FEM simulation in ANSYS.

After setting up a system of equations out of differential governing equation and boundary conditions through the process of discretization, presented numeric model pays back through its advantages. Firstly, recurrent equation written for all internal grid points that are not affected by discretized boundary conditions makes the model compact and convenient for development of software routines, e.g. in MATLAB. This feature opens additional possibilities for the research of the model behavior in variety of cases with different values of non-dimensional stiffness, mass and taper ratios. Therefore, presented approach with FDM provides us an excellent control of system parameters in particular engineering applications.

Finally, presented approach has great versatility and can be employed to solve an eigenvalue problem for the beam with any other type of cross-sectional variation and boundary conditions, without any limitations whatsoever.

ACKNOWLEDGMENT

This work was supported by the Ministry of Education, Science and Technological Development of the Republic of Serbia (Project TR35038).

REFERENCES

[1] Laura PAA, Gutierrez RH. Vibrations of an elastically restrained cantilever beam of varying cross-section with tip mass of finite length. Journal of Sound and Vibration 108(1), pp. 123–131, 1986.

[2] W.L. Craver Jr., P. Jampala. Transverse Vibrations of a Linearly Tapered Cantilever Beam With Constraining Springs. Journal of Sound and Vibration 166(3), pp. 521–529, 1993.

[3] R.O. Grossi, B. del V. Arenas. A variational approach to the vibration of tapered beams with elastically restrained ends. Journal of Sound and Vibration 195(3), pp. 507–511, 1996.

[4] N.M. Auciello. Transverse vibrations of a linearly tapered cantilever beam with tip mass of rotatory inertia and eccentricity. Journal of Sound and Vibration 194(1), pp. 25–34, 1996.

[5] N.M. Auciello, G. Nolè. Vibrations of a cantilever tapered beam with varying section properties and carrying a mass at the free end. Journal of Sound and Vibration 214(1), pp. 105–119, 1998.

[6] D. Zhou, Y.K. Cheung. The free vibration of a type of tapered beams. Computer Methods in Applied Mechanics and Engineering. 188, pp. 203–216, 2000.

[7] N.M. Auciello. On the transverse vibrations of non-uniform beams with axial loads and elastically restrained ends. International Journal of Mechanical Sciences 43, pp. 193–208, 2001.

[8] S. Naguleswaran. Vibration of an Euler–Bernoulli beam on elastic end supports and with up to three step changes in cross-section. International Journal of Mechanical Sciences 44, pp. 2541–2555, 2002.

[9] S. Naguleswaran. Vibration and stability of an Euler–Bernoulli beam with up to three-step changes in cross-section and in axial force. International Journal of Mechanical Sciences 45, pp. 1563–1579, 2003.

[10] Q.S. Li, L.F. Yang, Y.L. Zhao, G.Q. Li. Dynamic analysis of non-uniform beams and plates by finite elements with generalized degrees of freedom. International Journal of Mechanical Sciences 45, pp. 813–830, 2003.

[11] H. Qiao, Q.S. Li, G.Q. Li. Vibratory characteristics of flexural non-uniform Euler–Bernoulli beams carrying an arbitrary number of spring–mass systems. International Journal of Mechanical Sciences 44, pp. 725–743, 2002.

[12] Jong-Shyong Wu, Chin-Tzu Chen. An exact solution for the natural frequencies and mode shapes of an immersed elastically restrained wedge beam carrying an eccentric tip mass with mass moment of inertia. Journal of Sound and Vibration 286, pp. 549–568, 2005.

[13] Michael A. Koplow, Abhijit Bhattacharyya, Brian P. Mann. Closed form solutions for the dynamic response of Euler–Bernoulli beams with step changes in cross section. Journal of Sound and Vibration 295, pp. 214–225, 2006.

[14] R.D. Firouz-Abadi, H. Haddadpour, A.B. Novinzadeh. An asymptotic solution to transverse free vibrations of variable-section beams. Journal of Sound and Vibration 304, pp. 530–540, 2007.

[15] J.W. Jaworski, E.H. Dowell. Free vibration of a cantilevered beam with multiple steps: Comparison of several theoretical methods with experiment. Journal of Sound and Vibration 312, pp. 713–725, 2008.

[16] M.S. Abdel-Jaber et al. Nonlinear natural frequencies of an elastically restrained tapered beam. Journal of Sound and Vibration 313, pp. 772–783, 2008.

[17] Jung-Chang Hsu, Hsin-Yi Lai, C.K. Chen. Free vibration of non-uniform Euler–Bernoulli beams with general elastically end constraints using Adomian modified decomposition method. Journal of Sound and Vibration 318, pp. 965–981, 2008.

[18] E. J. Sapountzakis, D. G. Panagos. Nonlinear analysis of beams of variable cross section, including shear deformation effect. Archive of Applied Mechanics. 78, pp. 687–710, 2008.

[19] Yong Huang, Xian-Fang Li. A new approach for free vibration of axially functionally graded beams with non-uniform cross-section. Journal of Sound and Vibration 329, pp. 2291–2303, 2010.

[20] Korak Sarkar, Ranjan Ganguli. Closed-form solutions for non-uniform Euler–Bernoulli free–free beams. Journal of Sound and Vibration 332, pp. 6078–6092, 2013.

[21] S. Rajasekaran. Buckling and vibration of axially functionally graded nonuniform beams using differential transformation based dynamic stiffness approach. Meccanica 48, pp. 1053–1070, 2013.

[22] Samir AL-Sadder, Raid A. Othman AL-Rawi. Finite difference scheme for large-deflection analysis of non-prismatic cantilever beams subjected to different types of continuous and discontinuous loadings. Archive of Applied Mechanics 75, pp. 459–473, 2006.

[23] J. Awrejcewicz, A.V. Krysko, J. Mrozowski, O.A. Saltykova, M.V. Zhigalov. Analysis of regular and chaotic dynamics of the Euler–Bernoulli beams using finite difference and finite element methods. Acta Mechanica Sinica 27(1), pp. 36–43, 2011.

[24] Meirovitch L. Fundamentals of vibrations. McGraw-Hill, New York, 2001.

[25] Yong Huang, Ling-E Yang, Qi-Zhi Luo. Free vibration of axially functionally graded Timoshenko beams with non-uniform cross-section. Composites: Part B 45, pp. 1493–1498, 2013.

Table 1. First three circular natural frequencies obtained by FDM and FEM with relative deviations

		ω_1[rad/s]			ω_2[rad/s]			ω_3[rad/s]		
q	r	FDM	FEM	Δ_1	FDM	FEM	Δ_2	FDM	FEM	Δ_3
0.25	0.50	24.39	24.38	0.05%	367.67	364.12	0.97%	1299.50	1253.87	3.64%
	1.00	19.07	19.06	0.04%	347.28	343.99	0.96%	1278.50	1233.83	3.62%
	1.50	16.17	16.17	0.04%	339.32	336.13	0.95%	1270.90	1226.60	3.61%
	2.00	14.30	14.29	0.04%	335.08	331.93	0.95%	1267.00	1222.90	3.61%
0.50	0.50	32.99	32.97	0.06%	377.20	373.39	1.02%	1309.00	1262.42	3.69%
	1.00	25.72	25.70	0.06%	357.19	353.65	1.00%	1288.00	1242.44	3.67%
	1.50	21.79	21.78	0.06%	349.41	345.96	1.00%	1280.50	1235.27	3.66%
	2.00	19.24	19.23	0.06%	345.28	341.88	0.99%	1276.60	1231.57	3.66%
1.00	0.50	43.11	43.08	0.08%	393.78	389.48	1.10%	1326.60	1278.31	3.78%
	1.00	33.46	33.44	0.08%	374.30	370.28	1.08%	1305.80	1258.46	3.76%
	1.50	28.30	28.28	0.08%	366.77	362.87	1.08%	1298.30	1251.36	3.75%
	2.00	24.97	24.95	0.08%	362.79	358.93	1.07%	1294.50	1247.71	3.75%
1.50	0.50	49.30	49.26	0.10%	407.68	402.94	1.18%	1342.70	1292.70	3.87%
	1.00	38.15	38.11	0.10%	388.54	384.10	1.16%	1322.00	1272.97	3.85%
	1.50	32.22	32.19	0.09%	381.19	376.85	1.15%	1314.60	1265.87	3.85%
	2.00	28.41	28.38	0.09%	377.29	373.01	1.15%	1310.70	1262.23	3.84%
2.00	0.50	53.59	53.53	0.11%	419.51	414.36	1.24%	1357.30	1305.77	3.95%
	1.00	41.37	41.33	0.11%	400.59	395.75	1.22%	1336.70	1286.11	3.93%
	1.50	34.91	34.87	0.11%	393.34	388.62	1.22%	1329.30	1279.07	3.93%
	2.00	30.76	30.73	0.10%	389.51	384.85	1.21%	1325.50	1275.49	3.92%
3.00	0.50	59.22	59.14	0.13%	438.53	432.66	1.36%	1383.10	1328.52	4.11%
	1.00	45.57	45.52	0.12%	419.84	414.31	1.33%	1362.60	1309.04	4.09%
	1.50	38.40	38.36	0.12%	412.72	407.31	1.33%	1355.20	1302.06	4.08%
	2.00	33.81	33.77	0.12%	408.96	403.62	1.32%	1351.50	1298.48	4.08%
4.00	0.50	62.78	62.69	0.14%	453.13	446.67	1.45%	1404.90	1347.68	4.25%
	1.00	48.21	48.15	0.13%	434.54	428.44	1.42%	1384.40	1328.27	4.23%
	1.50	40.59	40.54	0.13%	427.47	421.51	1.41%	1377.10	1321.35	4.22%
	2.00	35.72	35.67	0.13%	423.75	417.86	1.41%	1373.40	1317.77	4.22%
5.00	0.50	65.24	65.14	0.15%	464.68	457.73	1.52%	1423.50	1363.95	4.37%
	1.00	50.03	49.96	0.14%	446.12	439.55	1.49%	1403.10	1344.60	4.35%
	1.50	42.10	42.04	0.14%	439.08	432.65	1.49%	1395.80	1337.69	4.34%
	2.00	37.03	36.98	0.14%	435.37	429.02	1.48%	1392.10	1334.11	4.35%
7.00	0.50	68.44	68.33	0.16%	481.78	474.05	1.63%	1453.60	1390.03	4.57%
	1.00	52.38	52.30	0.15%	463.19	455.88	1.60%	1433.30	1370.80	4.56%
	1.50	44.04	43.97	0.15%	456.16	449.00	1.60%	1426.00	1363.89	4.55%
	2.00	38.72	38.66	0.15%	452.47	445.38	1.59%	1422.30	1360.37	4.55%
9.00	0.50	70.42	70.30	0.17%	493.81	485.51	1.71%	1476.80	1410.01	4.74%
	1.00	53.83	53.75	0.16%	475.17	467.30	1.68%	1456.50	1390.78	4.73%
	1.50	45.24	45.16	0.16%	468.12	460.41	1.67%	1449.20	1383.93	4.72%
	2.00	39.76	39.70	0.16%	464.42	456.80	1.67%	1445.50	1380.42	4.71%
200.00	0.50	78.52	78.38	0.19%	557.89	546.22	2.14%	1634.70	1543.72	5.89%
	1.00	59.72	59.61	0.18%	538.40	527.32	2.10%	1613.90	1524.30	5.88%
	1.50	50.08	49.99	0.18%	531.10	520.23	2.09%	1606.40	1517.33	5.87%
	2.00	43.97	43.90	0.17%	527.27	516.52	2.08%	1602.60	1513.75	5.87%
10^6	0.50	78.97	78.83	0.18%	562.34	550.51	2.15%	1648.20	1555.34	5.97%
	1.00	60.04	59.94	0.17%	542.77	531.54	2.11%	1627.30	1535.80	5.96%
	1.50	50.34	50.26	0.17%	535.44	524.43	2.10%	1619.80	1528.89	5.95%
	2.00	44.20	44.13	0.17%	531.60	520.70	2.09%	1616.00	1525.31	5.95%
10^{12}	0.50	78.97	78.83	0.18%	562.34	550.51	2.15%	1648.20	1555.34	5.97%
	1.00	60.04	59.94	0.17%	542.77	531.54	2.11%	1627.30	1535.80	5.96%
	1.50	50.34	50.26	0.17%	535.44	524.43	2.10%	1619.80	1528.89	5.95%
	2.00	44.20	44.13	0.17%	531.60	520.70	2.09%	1616.00	1525.31	5.95%